Variability in Transient Climate Response in a large-ensemble global climate model simulation

B.K. Adams and A.E. Dessler

Abstract

The transient climate response (TCR), defined to be the warming in near-surface air temperature after 70 years of a 1% per year increase in CO_2, can be estimated from observed warming over the 19th and 20th centuries. Such analyses yield lower values than TCR estimated from global climate models (GCMs). This disagreement has been used to suggest that GCMs' climate may be too sensitive to increases in CO_2. Here we critically evaluate the methodology of the comparison using a large ensemble of a fully coupled GCM simulating the historical period, 1850–2005. We find that TCR estimated from model simulations of the historical period can be much lower than the model's true TCR, replicating the disagreement seen between observations and GCM estimates of TCR. This suggests that the disagreement could be explained entirely by the details of the comparison and undercuts the suggestions that GCMs overestimate TCR.

Introduction

The transient climate response (TCR) is frequently used to quantify the sensitivity of our climate system to increases in greenhouse gases. It is defined to be the warming in near-surface air temperature after 70 years of a 1% per year increase in atmospheric CO_2. As described below, it can be estimated from observed warming over the 19th and 20th centuries, yielding most-likely TCR values of 1.3-1.6 K [Bengtsson and Schwartz, 2013; Otto et al., 2013; Richardson et al., 2016; Lewis and Curry, 2018]. These values lie below the CMIP5 ensemble average TCR of 1.8 K [Forster *et al.*, 2013]. This disagreement has been used to cast doubt on the fidelity of model simulations of future climate change.

We will test the methodology of this comparison using a large model ensemble, an increasingly popular tool to study the impact of internal variability on the climate system. The most appropriate ensemble for this type of problem contains many runs of a single model with identical physics and external forcing but different initial conditions. As each ensemble member evolves in time, internal variability of the different members is out of phase, leading to differences in the climate states among the ensemble members. In fact, one can think of our observational record as one member of a theoretical ensemble of Earth's climate trajectories. A model ensemble therefore gives us insight into what alternative climate histories may have looked like.

Data

We analyze output from an ensemble of 100 runs of the fully-coupled Max Planck Institute Earth System Model version 1.1 (MPI-ESM1.1) covering the period 1850-2005. The ensemble was used by Dessler et al. [2018] to characterize the impact of internal variability on estimates of the equilibrium climate sensitivity (ECS); they found that internal variability can lead to significant errors in ECS inferred from historical observations. Hedemann et al. [2017] analyzed this ensemble to determine potential causes of the so-called warming hiatus that occurred in the 2000s.

This model consists of the ECHAM6.3 atmosphere and land model coupled to the MPI-OM ocean model. The atmospheric resolution is T63 spectral truncation, corresponding to about 200 km, with 47 vertical levels, whereas the ocean has a nominal resolution of about 1.5 degrees and 40 vertical levels. MPI-ESM1.1 is a bug-fixed and improved version of the MPI-ESM used for CMIP5 [Giorgetta *et al.*, 2013] and nearly identical to the MPI-ESM1.2 model being used to provide output to CMIP6, except that the historical forcing is from the MPI-ESM. Each of the 100 members simulates the years 1850-2005 and use the same evolution of historical natural and anthropogenic forcings. The members differ only in their initial conditions — each starts from a different state sampled from a 2000-year pre-industrial control simulation.

We calculate effective radiative forcing F for the ensemble by subtracting top-of-atmosphere flux R in a run with climatological sea surface temperatures (SSTs) and a constant pre-industrial atmosphere from average R in an ensemble of three runs using the same SSTs but the time-varying atmospheric composition used in the historical runs [Hansen *et al.*, 2005; Forster *et al.*, 2016]. The three-member ensemble begins with perturbed atmospheric states.

We estimate F_{2xCO2} using the same approach in a set of fixed SST runs, one with a pre-industrial atmosphere and one in which CO_2 increases at 1% per year. We estimate F_{2xCO2} as the average difference in top-of-atmosphere flux over years 62-78, which produces a value of 3.7 W/m^2. This is lower than the value used in Dessler et al. [2018], 3.9 W/m^2, which was estimated as one-half of the average over years 130-150. We feel the value of 3.7 W/m^2 is a more appropriate estimate of $2xCO_2$ forcing in this model.

We will also analyze a 68-member ensemble of the MPI-ESM1.1 forced with CO_2 increasing at 1%/year (hereafter, "1% runs"). As with the historical ensemble, the 1% ensemble members differ only in their initial conditions — each starts from a different state sampled from a 2000-year pre-industrial control simulation.

Analysis

Time series of global-average near-surface air temperature for all 100 members are plotted in Fig. 1 of Dessler et al. [2018]; that plot shows that the model ensemble is in good agreement with observed surface temperatures. TCR can be estimated from the ensemble's temperature data with this equation [Gregory and Forster, 2008; Otto *et al.*, 2013; Richardson *et al.*, 2016]:

$$\mathrm{TCR}_{hist} = \Delta\mathrm{T}\,\frac{\mathrm{F}_{2\times\mathrm{CO2}}}{\Delta\mathrm{F}} \qquad (1)$$

where ΔT is the change in temperature over the historical period and ΔF is the change in radiative forcing. In our analysis, Δ represents the change between the 1859-1882 average, selected because it is not strongly influenced by volcanic eruptions [Mauritsen and Pincus, 2017; Lewis and Curry, 2018], and the average of the last ten years of the runs, 1996-2005. We refer to TCRs estimated this way as TCR_{hist}.

We first calculate TCR_{hist} in each ensemble member using global-average near-surface air temperature for ΔT. The calculated values range from 1.32 to 1.94 K (5-95% range 1.48-1.90 K) (Fig. 1a, Table 1). The spread in these TCR estimates is entirely due to internal variability and it is similar to previous estimates [Huber *et al.*, 2014; Hawkins *et al.*, 2016]. The standard deviation of ΔT from the ensemble is 0.07 K, close to that assumed by Lewis and Curry [2015], implying a similar spread in TCR in their analysis.

TCR is formally defined as the warming of global-average near-surface air temperature in response to CO_2 increasing at 1% per year, at the time of doubling (year 70). This value, which we will call TCR_{true}, can be estimated by averaging the warming (relative to pre-industrial) in year 70 of the 68-member ensemble of 1% runs. We find that TCR_{true} for the MPI-ESM1.1 is 1.81 K; this is 0.13 K (7.6%) larger than the average of the ensemble's TCR_{hist} (1.68 K).

Thus, TCR_{hist} is a low-biased estimate of TCR_{true} in the ensemble. The magnitude, and even the sign, of this bias varies depending on the portion of the historical record being examined (Table 1). Overall, though, we see a clear tendency for the TCR_{hist} to underestimate TCR_{true} (Table 1). Previous papers have suggested that the biases in TCR_{hist} could be due to aerosol forcing efficacy [Kummer and Dessler, 2014; Shindell, 2014; Marvel *et al.*, 2015], although that explanation remains to be validated in this ensemble.

We are now in a position to critically evaluate previous comparisons of TCR from observations and GCMs. TCR estimated from observations, which are TCR_{hist}, have most-likely values in the range 1.3-1.6 K [Bengtsson and Schwartz, 2013; Otto *et al.*, 2013; Richardson *et al.*, 2016; Lewis and Curry, 2018], although the uncertainty in the individual estimates is large. The CMIP5 ensemble's TCR, which are TCR_{true}, fall in the range 1.8±0.6 K (average and 5-95% confidence interval) [Forster *et al.*, 2013]. Our analysis of the MPI-ESM1.1 ensemble demonstrates how a model with a TCR_{true} of 1.81 K might nevertheless produce TCR_{hist} in some ensemble members that that are much lower (1.3-1.4, Figure 1a) and in agreement with observational estimates. Thus, differences between observational TCRs and GCM TCRs could be mostly or entirely due to these issues.

We can also confirm previous suggestions that two issues with the observed ΔT, masking and blending, are further biasing TCR_{hist} to even lower values [Richardson *et al.*, 2016]. Masking refers to the fact that the observations are geographically incomplete, and that the degree of incompleteness has changed over time, leading to biases in global-average ΔT [Cowtan and Way, 2014]. To test the impact of this on TCR_{hist}, we also calculated ΔT in the ensemble using a time-varying mask derived from HadCRUT4 (v4.6.0.0) [Morice *et al.*, 2012]. Using this masked ΔT in Eq. 1, ensemble average TCR_{hist} drops from 1.68 K to 1.59 K (Fig. 1b, Table 2).

The second issue is blending, which refers to the fact that observed ΔT data sets are usually a blend of near-surface air temperature over land and sea ice but sea surface temperature (SST) over ocean. Because near-surface air temperature is warming faster than SSTs, this blending lowers ΔT compared to an estimate derived entirely from near-surface air temperature [Cowtan *et al.*, 2015; Santer *et al.*, 2000]. We test this by calculating a blended ΔT in the ensemble, which we also mask following HadCRUT4. Using this blended and masked ΔT, ensemble average TCR_{hist} drops to 1.47 K (Fig. 1d, Table 2). Importantly, none of the individual ensemble members have TCR_{hist} as large as the model's TCR_{true}.

Finally, we have also calculated blended ΔT using the temperature of the model's top ocean layer (representing the top 12 m of the ocean) instead of SST. Using that estimate of ΔT, TCR_{hist} drops even further, to an ensemble average of 1.44 K (Fig. 2f, Table 2).

Conclusions

We have investigated why observation-based estimates of TCR tend to be lower than those from GCMs. We have quantified a number of biases: 1) a bias between TCR_{hist} and TCR_{true}, 2) a bias due to incomplete spatial coverage in the observational ΔT record, and 3) a bias due to the observational ΔT values being blends of air temperature and SSTs. These three biases are all acting in the same direction, to push TCR_{hist} to lower values. The impact of internal variability, which can suppress warming in some members of the ensemble, thereby reducing TCR_{hist}, is not yet quantifiable. But it has a potentially large magnitude and therefore could also be playing a role in the model-observation difference.

The uncertainty in individual estimates of TCR_{hist} from observations are large and the range easily covers most of the TCR_{true} values from the CMIP5 ensemble [Lewis and Curry, 2015; Lewis and Curry, 2018; Richardson *et al.*, 2016]. Because of the large uncertainty in other parameters (e.g., aerosol forcing), adding uncertainty due to the issues we discuss in this paper will produce only nominal increases in the total uncertainty of the observational estimates. However, the biases we have investigated are capable of explaining most or all of the disagreement between the central values of the estimates, which has been the focus of much of the discussion.

Our work also informs how future analyses should be done. First, analyses should account for the role of internal variability, most likely by comparing observations to an ensemble of runs. In addition, we should not compare TCR_{hist} derived from observations to TCR_{true} — unless one can quantify and adjust for the bias between these methods. A better approach would be to compare TCR_{hist} from observations to TCR_{hist} derived from an ensemble of runs of the GCMs covering the same period as the observations. Finally, one must account for biases in the observations of ΔT due to masking and blending, most likely by calculating masked and blended ΔT fields from the model and using those to estimate the model-derived TCR_{hist}.

Acknowledgments: This work was supported by NSF grant AGS-1661861 to Texas A&M University. We thank the Bjorn Stevens, Thorsten Mauritsen, and Chris Hedemann of the Max-Planck-Institut für Meteorologie for their help interpreting output from the ensemble that formed the basis of this analysis. We also thank Mark Richardson for his suggestions on the manuscript. Data and code are available from [insert link after paper is accepted and code is finalized].

References

Bengtsson, L., & S. E. Schwartz (2013), Determination of a lower bound on Earth's climate sensitivity, Tellus B: Chemical and Physical Meteorology, 65, 21533, doi: 10.3402/tellusb.v65i0.21533.

Cowtan, K., & R. G. Way (2014), Coverage bias in the HadCRUT4 temperature series and its impact on recent temperature trends, Q. J. R. Meteor. Soc., 140, 1935-1944, doi: doi:10.1002/qj.2297.

Cowtan, K., Z. Hausfather, E. Hawkins, P. Jacobs, M. E. Mann, S. K. Miller, et al. (2015), Robust comparison of climate models with observations using blended land air and ocean sea surface temperatures, Geophys. Res. Lett., 42, 6526-6534, doi: 10.1002/2015GL064888.

Dessler, A. E., T. Mauritsen, & B. Stevens (2018), The influence of internal variability on Earth's energy balance framework and implications for estimating climate sensitivity, Atmos. Chem. Phys., 18, 5147-5155, doi: 10.5194/acp-18-5147-2018.

Forster, P. M., T. Andrews, P. Good, J. M. Gregory, L. S. Jackson, & M. Zelinka (2013), Evaluating adjusted forcing and model spread for historical and future scenarios in the CMIP5 generation of climate models, Journal of Geophysical Research: Atmospheres, 118, 1139-1150, doi: 10.1002/jgrd.50174.

Forster, P. M., T. Richardson, A. C. Maycock, C. J. Smith, B. H. Samset, G. Myhre, et al. (2016), Recommendations for diagnosing effective radiative forcing from climate models for CMIP6, J. Geophys. Res., 121, 12460-12475, doi: 10.1002/2016jd025320.
Giorgetta, M. A., J. Jungclaus, C. H. Reick, S. Legutke, J. Bader, M. Böttinger, et al. (2013), Climate and carbon cycle changes from 1850 to 2100 in MPI-ESM simulations for the Coupled Model Intercomparison Project phase 5, Journal of Advances in Modeling Earth Systems, 5, 572-597, doi: 10.1002/jame.20038.
Gregory, J. M., & P. M. Forster (2008), Transient climate response estimated from radiative forcing and observed temperature change, J. Geophys. Res., 113, doi: 10.1029/2008jd010405.
Hansen, J., M. Sato, R. Ruedy, L. Nazarenko, A. Lacis, G. A. Schmidt, et al. (2005), Efficacy of climate forcings, Journal of Geophysical Research: Atmospheres, 110, doi: 10.1029/2005JD005776.
Hawkins, E., R. S. Smith, J. M. Gregory, & D. A. Stainforth (2016), Irreducible uncertainty in near-term climate projections, Climate Dynamics, 46, 3807-3819, doi: 10.1007/s00382-015-2806-8.
Hedemann, C., T. Mauritsen, J. Jungclaus, & J. Marotzke (2017), The subtle origins of surface-warming hiatuses, Nature Clim. Change, 7, 336-339, doi: 10.1038/nclimate3274.
Huber, M., U. Beyerle, & R. Knutti (2014), Estimating climate sensitivity and future temperature in the presence of natural climate variability, Geophys. Res. Lett., 41, 2086-2092, doi: 10.1002/2013GL058532.
Kummer, J. R., & A. E. Dessler (2014), The impact of forcing efficacy on the equilibrium climate sensitivity, Geophys. Res. Lett., 41, 3565-3568, doi: 10.1002/2014gl060046.
Lewis, N., & J. A. Curry (2015), The implications for climate sensitivity of AR5 forcing and heat uptake estimates, Climate Dynamics, 45, 1009-1023, doi: 10.1007/s00382-014-2342-y.
Lewis, N., & J. Curry (2018), The impact of recent forcing and ocean heat uptake data on estimates of climate sensitivity, J. Climate, doi: 10.1175/jcli-d-17-0667.1.
Marvel, K., G. A. Schmidt, R. L. Miller, & L. S. Nazarenko (2015), Implications for climate sensitivity from the response to individual forcings, Nature Climate Change, 6, 386, doi: 10.1038/nclimate2888.
Mauritsen, T., & R. Pincus (2017), Committed warming inferred from observations, Nature Climate Change, 7, 652-655, doi: 10.1038/nclimate3357.
Morice, C. P., J. J. Kennedy, N. A. Rayner, & P. D. Jones (2012), Quantifying uncertainties in global and regional temperature change using an ensemble of observational estimates: The HadCRUT4 data set, J. Geophys. Res., 117, doi: 10.1029/2011jd017187.
Otto, A., F. E. L. Otto, O. Boucher, J. Church, G. Hegerl, P. M. Forster, et al. (2013), Energy budget constraints on climate response, Nature Geoscience, 6, 415-416, doi: 10.1038/ngeo1836.
Richardson, M., K. Cowtan, E. Hawkins, & M. B. Stolpe (2016), Reconciled climate response estimates from climate models and the energy budget of Earth, Nature Clim. Change, 6, 931-935, doi: 10.1038/nclimate3066.
Santer, B. D., T. M. L. Wigley, D. J. Gaffen, L. Bengtsson, C. Doutriaux, J. S. Boyle, et al. (2000), Interpreting differential temperature trends at the surface and in the lower troposphere, Science, 287, 1227.

Shindell, D. T. (2014), Inhomogeneous forcing and transient climate sensitivity, Nature Climate Change, 4, 274, doi: 10.1038/nclimate2136.

Table 1. TCR$_{hist}$ calculated with different base and end periods

base period	end period	average (K)	Full TCR range (K)	5-95% TCR range (K)	width (K)	% diff from true TCR	ΔF (W/m²)
1859-1882	1940-1949	1.82	0.63-2.88	1.15-2.50	1.35	0.4	0.54
1859-1882	1951-1960	1.96	1.10-3.13	1.32-2.67	1.34	7.6	0.59
1859-1882	1969-1978	1.71	1.01-2.91	1.24-2.24	0.99	-5.8	0.81
1859-1882	**1996-2005**	**1.68**	**1.32-1.94**	**1.48-1.90**	**0.42**	**-7.7**	**1.85**
1930-1939	1996-2005	1.65	0.97-2.07	1.35-1.99	0.64	-9.7	1.41
1940-1949	1996-2005	1.62	1.02-2.16	1.28-2.04	0.76	-11.5	1.31
1951-1960	1996-2005	1.55	0.91-2.04	1.20-1.90	0.70	-16.8	1.26
1970-1979	1996-2005	1.67	0.99-2.42	1.20-2.09	0.90	-8.5	0.99

The bold line is the case primarily discussed in the text. Width is the difference between the 5th and 95th percentile values; % difference is average TCR$_{hist}$ minus TCR$_{true}$, 1.81 K, divided by average TCR$_{hist}$,, in percent; ΔF is the change in forcing between the base and end periods.

Table 2. TCR$_{hist}$ calculated with different versions of ΔT

ΔT$_S$		average (K)	5-95% TCR range (K)	% diff from True TCR
TCR	**ΔT is global-average near-surface air temperature**	**1.68**	**1.48-1.90**	**-7.7**
TCR_masked	Same as TCR, but geographic coverage follows HadCRUT4	1.59	1.40-1.80	-13.7
TCR_blend	ΔT is a blend of near-surface air temperature over land and sea ice and SSTs over open ocean	1.56	1.37-1.77	-16.2
TCR_blend_masked	Same as TCR_blend, but geographic coverage follows HadCRUT4	1.47	1.28-1.67	-23.5
TCR_blend_oc	ΔT is a blend of near-surface air temperature over land and sea ice; elsewhere, use temperature of the top 12 m of the ocean	1.53	1.34-1.73	-18.6
TCR_blend_oc_masked	Same as TCR_blend_oc, but geographic coverage follows HadCRUT4	1.44	1.25-1.64	-25.8

The bold line is the base case primarily discussed in the text; % difference is average TCR$_{hist}$ minus TCR$_{true}$, 1.81 K, divided by average TCR$_{hist}$, in percent.

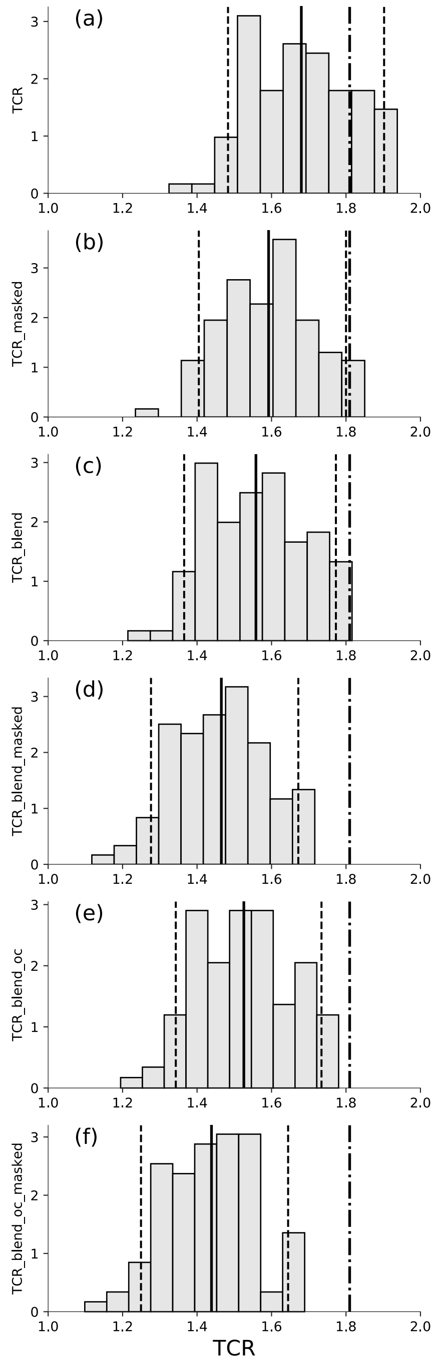

Figure 1. Histograms of TCR_{hist} (K) from the ensemble. Each panel shows the calculation with a different version of ΔT; see Table 2 for definitions. The solid black line represents the average, the dashed lines are the 5th and 95th percentiles. The dot-dashed line is TCR_{true} of the model, 1.81 K.